BABAR-PUB-04/06
SLAC-PUB-10439

A Measurement of the Total Width, the Electronic Width, and the Mass of the $\Upsilon(10580)$ Resonance

B. Aubert, R. Barate, D. Boutigny, F. Couderc, J.-M. Gaillard,
A. Hicheur, Y. Karyotakis, J. P. Lees, V. Tisserand, and A. Zghiche
Laboratoire de Physique des Particules, F-74941 Annecy-le-Vieux, France

A. Palano and A. Pompili
Università di Bari, Dipartimento di Fisica and INFN, I-70126 Bari, Italy

J. C. Chen, N. D. Qi, G. Rong, P. Wang, and Y. S. Zhu
Institute of High Energy Physics, Beijing 100039, China

G. Eigen, I. Ofte, and B. Stugu
University of Bergen, Inst. of Physics, N-5007 Bergen, Norway

G. S. Abrams, A. W. Borgland, A. B. Breon, D. N. Brown, J. Button-Shafer, R. N. Cahn, E. Charles,
C. T. Day, M. S. Gill, A. V. Gritsan, Y. Groysman, R. G. Jacobsen, R. W. Kadel, J. Kadyk, L. T. Kerth,
Yu. G. Kolomensky, G. Kukartsev, C. LeClerc, G. Lynch, A. M. Merchant, L. M. Mir, P. J. Oddone,
T. J. Orimoto, M. Pripstein, N. A. Roe, M. T. Ronan, V. G. Shelkov, A. V. Telnov, and W. A. Wenzel
Lawrence Berkeley National Laboratory and University of California, Berkeley, CA 94720, USA

K. Ford, T. J. Harrison, C. M. Hawkes, S. E. Morgan, and A. T. Watson
University of Birmingham, Birmingham, B15 2TT, United Kingdom

M. Fritsch, K. Goetzen, T. Held, H. Koch, B. Lewandowski, M. Pelizaeus, and M. Steinke
Ruhr Universität Bochum, Institut für Experimentalphysik 1, D-44780 Bochum, Germany

J. T. Boyd, N. Chevalier, W. N. Cottingham, M. P. Kelly, T. E. Latham, and F. F. Wilson
University of Bristol, Bristol BS8 1TL, United Kingdom

T. Cuhadar-Donszelmann, C. Hearty, T. S. Mattison, J. A. McKenna, and D. Thiessen
University of British Columbia, Vancouver, BC, Canada V6T 1Z1

P. Kyberd and L. Teodorescu
Brunel University, Uxbridge, Middlesex UB8 3PH, United Kingdom

V. E. Blinov, A. D. Bukin, V. P. Druzhinin, V. B. Golubev, V. N. Ivanchenko, E. A. Kravchenko,
A. P. Onuchin, S. I. Serednyakov, Yu. I. Skovpen, E. P. Solodov, and A. N. Yushkov
Budker Institute of Nuclear Physics, Novosibirsk 630090, Russia

D. Best, M. Bruinsma, M. Chao, I. Eschrich, D. Kirkby, A. J. Lankford,
M. Mandelkern, R. K. Mommsen, W. Roethel, and D. P. Stoker
University of California at Irvine, Irvine, CA 92697, USA

C. Buchanan and B. L. Hartfiel
University of California at Los Angeles, Los Angeles, CA 90024, USA

J. W. Gary, B. C. Shen, and K. Wang
University of California at Riverside, Riverside, CA 92521, USA

D. del Re, H. K. Hadavand, E. J. Hill, D. B. MacFarlane, H. P. Paar, Sh. Rahatlou, and V. Sharma

University of California at San Diego, La Jolla, CA 92093, USA

J. W. Berryhill, C. Campagnari, B. Dahmes, S. L. Levy,
O. Long, A. Lu, M. A. Mazur, J. D. Richman, and W. Verkerke
University of California at Santa Barbara, Santa Barbara, CA 93106, USA

T. W. Beck, A. M. Eisner, C. A. Heusch, W. S. Lockman, T. Schalk, R. E. Schmitz,
B. A. Schumm, A. Seiden, P. Spradlin, D. C. Williams, and M. G. Wilson
University of California at Santa Cruz, Institute for Particle Physics, Santa Cruz, CA 95064, USA

J. Albert, E. Chen, G. P. Dubois-Felsmann, A. Dvoretskii, D. G. Hitlin,
I. Narsky, T. Piatenko, F. C. Porter, A. Ryd, A. Samuel, and S. Yang
California Institute of Technology, Pasadena, CA 91125, USA

S. Jayatilleke, G. Mancinelli, B. T. Meadows, and M. D. Sokoloff
University of Cincinnati, Cincinnati, OH 45221, USA

T. Abe, F. Blanc, P. Bloom, S. Chen, P. J. Clark, W. T. Ford,
U. Nauenberg, A. Olivas, P. Rankin, J. G. Smith, and L. Zhang
University of Colorado, Boulder, CO 80309, USA

A. Chen, J. L. Harton, A. Soffer, W. H. Toki, R. J. Wilson, and Q. L. Zeng
Colorado State University, Fort Collins, CO 80523, USA

D. Altenburg, T. Brandt, J. Brose, T. Colberg, M. Dickopp, E. Feltresi, A. Hauke,
H. M. Lacker, E. Maly, R. Müller-Pfefferkorn, R. Nogowski, S. Otto, A. Petzold,
J. Schubert, K. R. Schubert, R. Schwierz, B. Spaan, and J. E. Sundermann
Technische Universität Dresden, Institut für Kern- und Teilchenphysik, D-01062 Dresden, Germany

D. Bernard, G. R. Bonneaud, F. Brochard, P. Grenier, S. Schrenk, Ch. Thiebaux, G. Vasileiadis, and M. Verderi
Ecole Polytechnique, LLR, F-91128 Palaiseau, France

D. J. Bard, A. Khan, D. Lavin, F. Muheim, and S. Playfer
University of Edinburgh, Edinburgh EH9 3JZ, United Kingdom

M. Andreotti, V. Azzolini, D. Bettoni, C. Bozzi, R. Calabrese,
G. Cibinetto, E. Luppi, M. Negrini, L. Piemontese, and A. Sarti
Università di Ferrara, Dipartimento di Fisica and INFN, I-44100 Ferrara, Italy

E. Treadwell
Florida A&M University, Tallahassee, FL 32307, USA

R. Baldini-Ferroli, A. Calcaterra, R. de Sangro, G. Finocchiaro, P. Patteri, M. Piccolo, and A. Zallo
Laboratori Nazionali di Frascati dell'INFN, I-00044 Frascati, Italy

A. Buzzo, R. Capra, R. Contri, G. Crosetti, M. Lo Vetere, M. Macri,
M. R. Monge, S. Passaggio, C. Patrignani, E. Robutti, A. Santroni, and S. Tosi
Università di Genova, Dipartimento di Fisica and INFN, I-16146 Genova, Italy

S. Bailey, G. Brandenburg, M. Morii, and E. Won
Harvard University, Cambridge, MA 02138, USA

R. S. Dubitzky and U. Langenegger
Universität Heidelberg, Physikalisches Institut, Philosophenweg 12, D-69120 Heidelberg, Germany

W. Bhimji, D. A. Bowerman, P. D. Dauncey, U. Egede, J. R. Gaillard, G. W. Morton, J. A. Nash, and G. P. Taylor
Imperial College London, London, SW7 2AZ, United Kingdom

G. J. Grenier and U. Mallik
University of Iowa, Iowa City, IA 52242, USA

J. Cochran, H. B. Crawley, J. Lamsa, W. T. Meyer, S. Prell, E. I. Rosenberg, and J. Yi
Iowa State University, Ames, IA 50011-3160, USA

M. Davier, G. Grosdidier, A. Höcker, S. Laplace, F. Le Diberder, V. Lepeltier,
A. M. Lutz, T. C. Petersen, S. Plaszczynski, M. H. Schune, L. Tantot, and G. Wormser
Laboratoire de l'Accélérateur Linéaire, F-91898 Orsay, France

C. H. Cheng, D. J. Lange, M. C. Simani, and D. M. Wright
Lawrence Livermore National Laboratory, Livermore, CA 94550, USA

A. J. Bevan, J. P. Coleman, J. R. Fry, E. Gabathuler, R. Gamet,
R. J. Parry, D. J. Payne, R. J. Sloane, and C. Touramanis
University of Liverpool, Liverpool L69 72E, United Kingdom

J. J. Back, C. M. Cormack, P. F. Harrison,* and G. B. Mohanty
Queen Mary, University of London, E1 4NS, United Kingdom

C. L. Brown, G. Cowan, R. L. Flack, H. U. Flaecher, M. G. Green, C. E. Marker,
T. R. McMahon, S. Ricciardi, F. Salvatore, G. Vaitsas, and M. A. Winter
University of London, Royal Holloway and Bedford New College, Egham, Surrey TW20 0EX, United Kingdom

D. Brown and C. L. Davis
University of Louisville, Louisville, KY 40292, USA

J. Allison, N. R. Barlow, R. J. Barlow, P. A. Hart, M. C. Hodgkinson, G. D. Lafferty, A. J. Lyon, and J. C. Williams
University of Manchester, Manchester M13 9PL, United Kingdom

A. Farbin, W. D. Hulsbergen, A. Jawahery, D. Kovalskyi, C. K. Lae, V. Lillard, and D. A. Roberts
University of Maryland, College Park, MD 20742, USA

G. Blaylock, C. Dallapiccola, K. T. Flood, S. S. Hertzbach, R. Kofler,
V. B. Koptchev, T. B. Moore, S. Saremi, H. Staengle, and S. Willocq
University of Massachusetts, Amherst, MA 01003, USA

R. Cowan, G. Sciolla, F. Taylor, and R. K. Yamamoto
Massachusetts Institute of Technology, Laboratory for Nuclear Science, Cambridge, MA 02139, USA

D. J. J. Mangeol, P. M. Patel, and S. H. Robertson
McGill University, Montréal, QC, Canada H3A 2T8

A. Lazzaro and F. Palombo
Università di Milano, Dipartimento di Fisica and INFN, I-20133 Milano, Italy

J. M. Bauer, L. Cremaldi, V. Eschenburg, R. Godang, R. Kroeger,
J. Reidy, D. A. Sanders, D. J. Summers, and H. W. Zhao
University of Mississippi, University, MS 38677, USA

S. Brunet, D. Côté, and P. Taras
Université de Montréal, Laboratoire René J. A. Lévesque, Montréal, QC, Canada H3C 3J7

H. Nicholson
Mount Holyoke College, South Hadley, MA 01075, USA

N. Cavallo, F. Fabozzi,† C. Gatto, L. Lista, D. Monorchio, P. Paolucci, D. Piccolo, and C. Sciacca
Università di Napoli Federico II, Dipartimento di Scienze Fisiche and INFN, I-80126, Napoli, Italy

M. Baak, H. Bulten, G. Raven, and L. Wilden
NIKHEF, National Institute for Nuclear Physics and High Energy Physics, NL-1009 DB Amsterdam, The Netherlands

C. P. Jessop and J. M. LoSecco
University of Notre Dame, Notre Dame, IN 46556, USA

T. A. Gabriel
Oak Ridge National Laboratory, Oak Ridge, TN 37831, USA

T. Allmendinger, B. Brau, K. K. Gan, K. Honscheid, D. Hufnagel, H. Kagan,
R. Kass, T. Pulliam, A. M. Rahimi, R. Ter-Antonyan, and Q. K. Wong
Ohio State University, Columbus, OH 43210, USA

J. Brau, R. Frey, O. Igonkina, C. T. Potter, N. B. Sinev, D. Strom, and E. Torrence
University of Oregon, Eugene, OR 97403, USA

F. Colecchia, A. Dorigo, F. Galeazzi, M. Margoni, M. Morandin,
M. Posocco, M. Rotondo, F. Simonetto, R. Stroili, G. Tiozzo, and C. Voci
Università di Padova, Dipartimento di Fisica and INFN, I-35131 Padova, Italy

M. Benayoun, H. Briand, J. Chauveau, P. David, Ch. de la Vaissière, L. Del Buono, O. Hamon,
M. J. J. John, Ph. Leruste, J. Ocariz, M. Pivk, L. Roos, S. T'Jampens, and G. Therin
Universités Paris VI et VII, Lab de Physique Nucléaire H. E., F-75252 Paris, France

P. F. Manfredi and V. Re
Università di Pavia, Dipartimento di Elettronica and INFN, I-27100 Pavia, Italy

P. K. Behera, L. Gladney, Q. H. Guo, and J. Panetta
University of Pennsylvania, Philadelphia, PA 19104, USA

F. Anulli and I. M. Peruzzi
Laboratori Nazionali di Frascati dell'INFN, I-00044 Frascati, Italy and
Università di Perugia, Dipartimento di Fisica and INFN, I-06100 Perugia, Italy

M. Biasini and M. Pioppi
Università di Perugia, Dipartimento di Fisica and INFN, I-06100 Perugia, Italy

C. Angelini, G. Batignani, S. Bettarini, M. Bondioli, F. Bucci, G. Calderini, M. Carpinelli,
V. Del Gamba, F. Forti, M. A. Giorgi, A. Lusiani, G. Marchiori, F. Martinez-Vidal,[‡]
M. Morganti, N. Neri, E. Paoloni, M. Rama, G. Rizzo, F. Sandrelli, and J. Walsh
Università di Pisa, Dipartimento di Fisica, Scuola Normale Superiore and INFN, I-56127 Pisa, Italy

M. Haire, D. Judd, K. Paick, and D. E. Wagoner
Prairie View A&M University, Prairie View, TX 77446, USA

N. Danielson, P. Elmer, C. Lu, V. Miftakov, J. Olsen, and A. J. S. Smith
Princeton University, Princeton, NJ 08544, USA

F. Bellini, R. Faccini, F. Ferrarotto, F. Ferroni, M. Gaspero, L. Li Gioi,
M. A. Mazzoni, S. Morganti, M. Pierini, G. Piredda, F. Safai Tehrani, and C. Voena
Università di Roma La Sapienza, Dipartimento di Fisica and INFN, I-00185 Roma, Italy

G. Cavoto
Princeton University, Princeton, NJ 08544, USA and
Università di Roma La Sapienza, Dipartimento di Fisica and INFN, I-00185 Roma, Italy

S. Christ, G. Wagner, and R. Waldi
Universität Rostock, D-18051 Rostock, Germany

T. Adye, N. De Groot, B. Franek, N. I. Geddes, G. P. Gopal, and E. O. Olaiya
Rutherford Appleton Laboratory, Chilton, Didcot, Oxon, OX11 0QX, United Kingdom

R. Aleksan, S. Emery, A. Gaidot, S. F. Ganzhur, P.-F. Giraud, G. Hamel de Monchenault, W. Kozanecki, M. Langer, M. Legendre, G. W. London, B. Mayer, G. Schott, G. Vasseur, Ch. Yèche, and M. Zito
DSM/Dapnia, CEA/Saclay, F-91191 Gif-sur-Yvette, France

M. V. Purohit, A. W. Weidemann, and F. X. Yumiceva
University of South Carolina, Columbia, SC 29208, USA

D. Aston, R. Bartoldus, N. Berger, A. M. Boyarski, O. L. Buchmueller, M. R. Convery, M. Cristinziani, G. De Nardo, M. Donald, D. Dong, J. Dorfan, D. Dujmic, W. Dunwoodie, E. E. Elsen, S. Fan, R. C. Field, A. Fisher, T. Glanzman, S. J. Gowdy, T. Hadig, V. Halyo, C. Hast, T. Hryn'ova, W. R. Innes, M. H. Kelsey, P. Kim, M. L. Kocian, D. W. G. S. Leith, J. Libby, S. Luitz, V. Luth, H. L. Lynch, H. Marsiske, R. Messner, D. R. Muller, C. P. O'Grady, V. E. Ozcan, A. Perazzo, M. Perl, S. Petrak, B. N. Ratcliff, A. Roodman, A. A. Salnikov, R. H. Schindler, J. Schwiening, J. Seeman, G. Simi, A. Snyder, A. Soha, J. Stelzer, D. Su, M. K. Sullivan, J. Va'vra, S. R. Wagner, M. Weaver, A. J. R. Weinstein, U. Wienands, W. J. Wisniewski, M. Wittgen, D. H. Wright, A. K. Yarritu, and C. C. Young
Stanford Linear Accelerator Center, Stanford, CA 94309, USA

P. R. Burchat, A. J. Edwards, T. I. Meyer, B. A. Petersen, and C. Roat
Stanford University, Stanford, CA 94305-4060, USA

S. Ahmed, M. S. Alam, J. A. Ernst, M. A. Saeed, M. Saleem, and F. R. Wappler
State Univ. of New York, Albany, NY 12222, USA

W. Bugg, M. Krishnamurthy, and S. M. Spanier
University of Tennessee, Knoxville, TN 37996, USA

R. Eckmann, H. Kim, J. L. Ritchie, A. Satpathy, and R. F. Schwitters
University of Texas at Austin, Austin, TX 78712, USA

J. M. Izen, I. Kitayama, X. C. Lou, and S. Ye
University of Texas at Dallas, Richardson, TX 75083, USA

F. Bianchi, M. Bona, F. Gallo, and D. Gamba
Università di Torino, Dipartimento di Fisica Sperimentale and INFN, I-10125 Torino, Italy

C. Borean, L. Bosisio, C. Cartaro, F. Cossutti, G. Della Ricca, S. Dittongo, S. Grancagnolo, L. Lanceri, P. Poropat,[§] L. Vitale, and G. Vuagnin
Università di Trieste, Dipartimento di Fisica and INFN, I-34127 Trieste, Italy

R. S. Panvini
Vanderbilt University, Nashville, TN 37235, USA

Sw. Banerjee, C. M. Brown, D. Fortin, P. D. Jackson, R. Kowalewski, and J. M. Roney
University of Victoria, Victoria, BC, Canada V8W 3P6

H. R. Band, S. Dasu, M. Datta, A. M. Eichenbaum, J. J. Hollar, J. R. Johnson, P. E. Kutter, H. Li, R. Liu, F. Di Lodovico, A. Mihalyi, A. K. Mohapatra, Y. Pan, R. Prepost, S. J. Sekula, P. Tan, J. H. von Wimmersperg-Toeller, J. Wu, S. L. Wu, and Z. Yu
University of Wisconsin, Madison, WI 53706, USA

H. Neal
Yale University, New Haven, CT 06511, USA

(Dated: February 7, 2008)

We present a measurement of the parameters of the $\Upsilon(10580)$ resonance based on a dataset

collected with the *BABAR* detector at the SLAC PEP-II asymmetric B factory. We measure the total width $\Gamma_{\rm tot} = (20.7 \pm 1.6 \pm 2.5)$ MeV, the electronic partial width $\Gamma_{ee} = (0.321 \pm 0.017 \pm 0.029)$ keV and the mass $M = (10579.3 \pm 0.4 \pm 1.2)$ MeV/c^2.

PACS numbers: 13.25.Gv, 14.40.Gx

I. INTRODUCTION

The $\Upsilon(10580)$ resonance is the lowest mass $b\bar{b}$ vector state above open-bottom threshold that decays into two B mesons. The total decay width $\Gamma_{\rm tot}$ of the $\Upsilon(10580)$ is therefore much larger than the widths of the lower mass Υ states, thereby allowing a direct measurement of $\Gamma_{\rm tot}$ at an e^+e^- collider. Although the state has been known for almost 20 years, its mass and width have been known only with relatively large uncertainties, and with central values from different experiments showing substantial variation [1–4]. We present new measurements of the mass, the total width, and the electronic widths of the $\Upsilon(10580)$ with improved precision.

II. EXPERIMENT AND DATA

The data used in this analysis were collected with the *BABAR* detector at the PEP-II storage ring [5]. The data set comprises three energy scans of the $\Upsilon(10580)$ and one scan of the $\Upsilon(3S)$ resonance. The PEP-II B factory is a high-luminosity asymmetric e^+e^- collider designed to operate at a center-of-mass (CM) energy around 10.58 GeV.

The PEP-II energy is calculated from the values of the currents of the power supplies for the magnets in the ring. Every major magnet in the ring has been measured in the laboratory and a current (I) vs. magnetic field (B) curve is determined for each magnet. The curve is a 4th order polynomial fit to the measured data. Many of the ring magnets are connected in series as strings with a single power supply. For the high-energy ring (HER) the bend magnets are in two strings of 96 magnets each. The I vs. B curve for a particular magnet string is then the average of the measured curves of the magnets in the string. The HER bend magnets are sorted according to field strength at a fixed I so that we have the following layout: high-medium-low then low-medium-high [6]. The power supplies are controlled by zero-flux transductors with each supply having a primary and a secondary transductor. The transductor accuracy is on the order of 10^{-5} and the secondary transductor is used to check the primary transductor.

When an energy scan is being made the CM energy is changed by changing the energy of the high-energy beam, while the low-energy beam is left unchanged. The energy of the HER is adjusted by increasing the current in all of the large magnet power supplies (main dipoles and all quadrupoles but no skew quadrupoles) by a calibrated amount based on the I vs. B curves for the power supplies. The small orbit-correctors in the beam are not changed. The beam orbit is monitored to ensure the orbit is not changing during an energy scan. Other variables that affect the beam energy via the RF frequency are also held constant. In the first energy scan PEP-II experienced problems with one or more RF stations in the HER. These stations (of which there were five at the time) add discrete amounts of energy to the beam at the location of the RF station to compensate for the beam-energy loss due to synchrotron radiation emission around the ring. If one or more stations are off due to problems, the actual beam energy at the collision point can change by a small amount, which depends on the station that was turned off [7].

In order to minimize magnet hysteresis effects, the ring magnets are standardized by ramping the magnets to a maximum current setting, then to zero current four times. This was also done before the I vs. B curves were measured as a function of increasing magnetic field. The ring energy is lowered to the lowest energy point of the scan and then the magnets are standardized. Energy scans are always done in the direction of increasing magnetic field.

BABAR is a solenoidal detector optimized for the asymmetric beam configuration at PEP-II. Charged-particle momenta are measured in a tracking system consisting of a five-layer, double-sided silicon vertex tracker (SVT) and a 40-layer drift chamber (DCH) filled with a mixture of helium and isobutane, operating in a 1.5-T superconducting solenoidal magnet. The electromagnetic calorimeter (EMC) consists of 6580 CsI(Tl) crystals arranged in a barrel and forward endcap. A detector of internally reflected Cherenkov light (DIRC) provides separation of pions, kaons and protons. Muons and long-lived neutral hadrons are identified in the instrumented flux return (IFR), composed of resistive plate chambers and layers of iron. A detailed description of the detector can be found in Ref. [8].

III. RESONANCE SHAPE

The $\Upsilon(10580)$ resonance parameters can be determined by measuring the energy dependence of the cross section $\sigma_{b\bar{b}}$ of the reaction $e^+e^- \to \Upsilon(10580) \to B\overline{B}$ in an en-

*Now at Department of Physics, University of Warwick, Coventry, United Kingdom
†Also with Università della Basilicata, Potenza, Italy
‡Also with IFIC, Instituto de Física Corpuscular, CSIC-Universidad de Valencia, Valencia, Spain
§Deceased

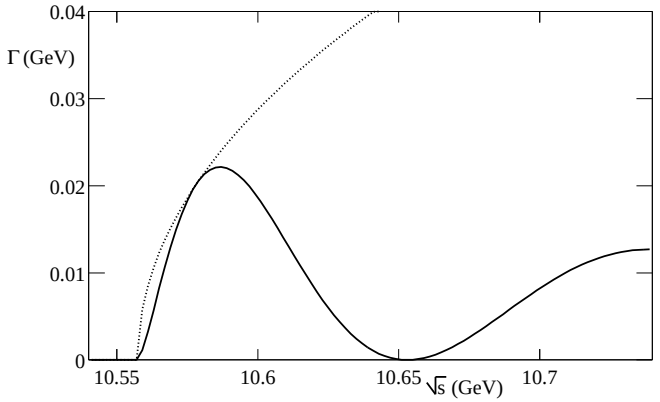

FIG. 1: The decay width $\Gamma_{\Upsilon(4S)\to B\overline{B}}(s)$ for the QPC model (solid line) compared to phase space alone (dotted line). Due to the proximity to the threshold, the width rises steeply. However, the overlap integral of the 4S Upsilon state with the 1S B-meson states vanishes three times due to the nodes of the 4S wave function, and pushes $\Gamma(s)$ down.

ergy interval around the resonance mass. The cross section of this process, neglecting radiative corrections and the beam-energy spread, is given by a relativistic Breit-Wigner function

$$\sigma_0(s) = 12\pi \frac{\Gamma^0_{ee}\Gamma_{\rm tot}(s)}{(s-M^2)^2 + M^2\Gamma^2_{\rm tot}(s)}, \qquad (1)$$

where Γ^0_{ee} is the partial decay width into e^+e^-, $\Gamma_{\rm tot}$ is the total decay width, M is the mass of the resonance, and $\sqrt{s}$ is the CM energy of the e^+e^- collision. The partial decay width Γ^0_{ee} is taken as constant and the approximation $\Gamma_{\rm tot}(s) \approx \Gamma_{\Upsilon(4S)\to B\overline{B}}(s)$ is used.

Since the $\Upsilon(10580)$ is so close to the threshold for $B\overline{B}$ production, its width $\Gamma_{\rm tot}(s)$ is expected to vary strongly with energy $\sqrt{s}$. It rises from zero at $\sqrt{s} = 2m_B$, but its behavior beyond that depends on decay dynamics. The quark-pair-creation model (QPCM) [9] is used to describe these dynamics. It is a straightforward model where the b and $\bar{b}$ quarks from the bound state, together with a quark-antiquark pair created from the vacuum, combine to form a $\overline{B}$ and a B meson. The matrix element for this decay is given by a spin-dependent amplitude and an overlap integral of the $\Upsilon(10580)$, treated as a pure $4S$ state.

$$\Gamma_{\Upsilon(4S)\to B\overline{B}}(s) = \frac{1}{8\pi}\left| g_{BB\Upsilon} \sum_{m=\pm1} I_4(m,\boldsymbol{q}) \right|^2 \frac{q(s)}{s} \qquad (2)$$

where m is the 3-component of the Υ spin. The overlap integral of the $\Upsilon(nS)$ state with two B mesons

$$I_n(m,\boldsymbol{q}) = \int Y_1^m(2\boldsymbol{q}-\boldsymbol{Q})\,\psi_{\Upsilon(nS)}(\boldsymbol{Q})\,\psi_B(\boldsymbol{Q}-h\boldsymbol{q}) \times \times \psi_{\overline{B}}(-\boldsymbol{Q}+h\boldsymbol{q})\,{\rm d}^3Q \qquad (3)$$

where $\boldsymbol{q}$ is the momentum vector of the B meson, and $h = 2m_b/(m_b+m_q)$ [10]. The calculation based on the harmonic oscillator wave function

$$\psi(\boldsymbol{q}) = \left(\frac{R^2}{\pi}\right)^{\frac{3}{4}} e^{-R^2q^2/8}$$

for the 1S state yields

$$I_4(m,\boldsymbol{q}) = \sqrt{\frac{1}{35}}\Bigg[\ 14R^2\frac{\partial}{\partial R^2} + 16R^4\left(\frac{\partial}{\partial R^2}\right)^2 + \frac{16}{3}R^6\left(\frac{\partial}{\partial R^2}\right)^3\Bigg] I_1(m,\boldsymbol{q}) \qquad (4)$$

with $R = R_{\Upsilon(4S)}$ and

$$I_1(m,\boldsymbol{q}) = \frac{8\sqrt{6}}{\pi^2}\left(\frac{RR_B^2}{R^2+2R_B^2}\right)^{3/2}\left(1-\frac{hR_B^2}{R^2+2R_B^2}\right)\times \times \exp\left(-\frac{R^2R_B^2h^2q^2}{4(R^2+2R_B^2)}\right)\boldsymbol{\epsilon}(m)\cdot\boldsymbol{q} \qquad (5)$$

We use the approximation with harmonic-oscillator wave functions provided by the ARGUS collaboration [1], i.e., the Hamiltonian

$$\mathcal{H} = m_b + m_q - \frac{(m_b+m_q)\nabla^2}{2m_bm_q} + 0.186\,{\rm GeV}^2 r - \frac{4\alpha_s}{3\,r} - 0.802\,{\rm GeV} \qquad (6)$$

with $\alpha_s = 0.35(0.42)$ for the $\Upsilon(4S)$ (B), $m_b = 5.17\,{\rm GeV}$ and $m_q = 0.33\,{\rm GeV}$, where they obtain as a minimum of $\langle\psi|\mathcal{H}|\psi\rangle$ the values $R = R_{\Upsilon(4S)} = 1.707\,{\rm GeV}^{-1}$, $R_B = 2.478\,{\rm GeV}^{-1}$. The resulting $\Gamma_{\Upsilon(4S)\to B\overline{B}}(s)$ is shown in Figure 1 and compared to the behaviour of spin-0 point-like particles. The fact that the Υ- and B-mesons are extended objects modifies the shape significantly.

The uncertainty of this model is parametrized as one constant $g_{BB\Upsilon}$, representing the coupling of the $\Upsilon(4S)$ to a $B\overline{B}$ pair, and is absorbed in the fit to the data by the free total width $\Gamma_{\rm tot} = \Gamma(M^2)$, assuming $\Gamma_{\rm tot} \approx \Gamma_{B\overline{B}}$. The free parameters of this model are hence the mass M and the width $\Gamma_{\rm tot}$.

The resonance shape is significantly modified by QED corrections [11, 12]. The cross section including radiative corrections of $O(\alpha^3)$ is given by

$$\tilde{\sigma}(s) = \int_0^{1-4m_e^2/s} \sigma_0(s-s\kappa)\beta\kappa^{\beta-1}(1+\delta_{\rm vert}+\delta_{\rm vac})\,{\rm d}\kappa, \qquad (7)$$

where $\kappa = \frac{2E_\gamma}{\sqrt{s}}$ is the scaled energy of the radiated photon, $\beta = \frac{2\alpha}{\pi}(\ln\frac{s}{m_e^2}-1)$, and $\delta_{\rm vert} = \frac{2\alpha}{\pi}(\frac{3}{4}\ln\frac{s}{m_e^2} - 1 + \frac{\pi^2}{6})$ is the vertex correction. The vacuum polarization of the photon propagator $\delta_{\rm vac}$ is absorbed in the physical partial width $\Gamma_{ee} \approx \Gamma^0_{ee}(1+\delta_{\rm vac})$ [13].

A second modification of the cross section arises from the beam-energy spread of PEP-II. Averaging over the

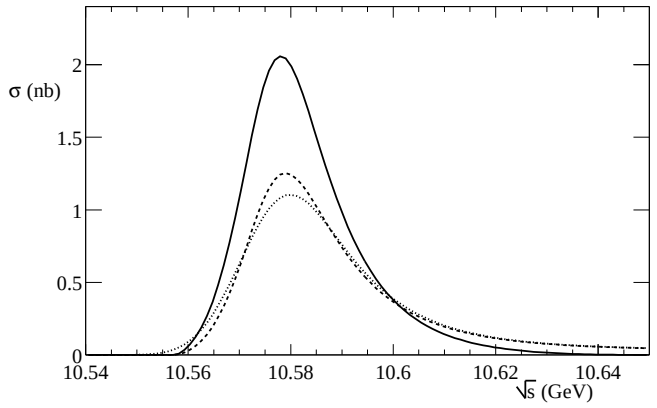

FIG. 2: Cross section without (solid line) and including (dashed line) initial photon radiation. Further broadening from the beam energy spread leads to the shape given by the dotted line.

e^+e^- CM energies $\sqrt{s'}$, which are assumed to have a Gaussian distribution around the mean value $\sqrt{s}$ with a standard deviation Δ, results in a cross section of:

$$\sigma_{b\overline{b}}(s) = \int \tilde{\sigma}(s')\frac{1}{\sqrt{2\pi}\Delta}\exp\left(-\frac{(\sqrt{s'}-\sqrt{s})^2}{2\Delta^2}\right)\mathrm{d}\sqrt{s'}. \tag{8}$$

Extraction of $\Gamma_{\rm tot}$ from the observed resonance shape requires knowledge of the energy spread Δ. The spread is measured from a scan of the narrow $\Upsilon(3S)$ resonance. Both effects are illustrated in Figure 2.

IV. DATA ANALYSIS

The strategy of this analysis is to determine the shape of the $\Upsilon(10580)$ resonance from three energy scans in which the cross section is measured from small data samples at several CM energies near the resonance. These are combined with a precise measurement of the peak cross section from a high-statistics data set with a well understood detector efficiency taken close to the peak in the course of B-meson data accumulation.

A. Event Selection

The visible hadronic cross section measured from the number of hadronic events $N_{\rm had}$ and the luminosity L is related to $\sigma_{b\overline{b}}$ via

$$\sigma^{\rm vis}(s) \equiv \frac{N_{\rm had}}{L} = \varepsilon_{b\overline{b}}\sigma_{b\overline{b}}(s) + \frac{P}{s}, \tag{9}$$

where $\varepsilon_{b\overline{b}}$ is the detection efficiency for $\Upsilon(10580) \to B\overline{B}$. The parameter P describes the amount of background from non-$B\overline{B}$ events, which are dominantly $e^+e^- \to q\bar{q}$.

Any selection of hadronic events will have backgrounds from two classes of sources. Processes such as $e^+e^- \to q\overline{q}(\gamma)$, $e^+e^- \to e^+e^-e^+e^-$ or $e^+e^- \to \tau^+\tau^-(\gamma)$ all have cross sections $\sigma \propto 1/s$ with corrections that are negligible over the limited energy range of each scan. This permits describing this class of backgrounds in a fit to the data by one parameter P. The second class of backgrounds originates from two-photon processes $\gamma\gamma \to$ hadrons or beam-gas interactions, which do not scale in a simple way with energy. The latter process even depends on the vacuum in the beam pipe rather than on the beam energy. This kind of background cannot be taken into account in the fit of the resonance. Therefore the event selection must reduce this background to a negligible level.

Hadronic events are selected by exploiting the fact that they have a higher charged-track multiplicity $N_{\rm ch}$ and have an event-shape that is more spherical than background events. Charged tracks are required to originate from the beam-crossing region and the event shape is measured with the normalized second Fox-Wolfram moment R_2 [14]. Additional selection criteria are applied to reduce the beam-gas and $\gamma\gamma$ backgrounds. The particular criteria for the analysis of the $\Upsilon(3S)$ scan data, the peak cross section measurement, and the $\Upsilon(10580)$ scan are described in the paragraphs below.

B. Luminosity Determination

The luminosity is measured from $e^+e^- \to \mu^+\mu^-$ events. These events are required to have at least one pair of charged tracks with an invariant mass greater than $7.5\,\mathrm{GeV}/c^2$. The acolinearity angle between these tracks in the CM has to be smaller than 10 degrees to reject cosmic rays. At least one of the tracks must have associated energy deposited in the calorimeter. Bhabha events are vetoed by requiring that none of the tracks has an associated energy deposited in the calorimeter of more than 1 GeV.

C. Calibration Using the $\Upsilon(3S)$ Resonance

The $\Upsilon(3S)$ scan taken in November 2002 consists of ten cross section measurements performed at different CM energies. The energies are obtained from the settings of the PEP-II storage ring. The visible cross section $\sigma_{\rm vis}$ is measured for each energy. The $\Upsilon(3S)$ decays have higher multiplicity and are more isotropic than the continuum background, which allows us to select $\Upsilon(3S)$ events with requirements similar to those used for the $B\overline{B}$ selection. In particular, the criteria $R_2 < 0.4$ and $N_{\rm ch} \geq 3$ are used to select hadronic events. Additionally, the invariant mass of all tracks combined is required to be greater than $2.2\ \mathrm{GeV}/c^2$.

The branching fraction of the $\Upsilon(3S)$ into $\mu^+\mu^-$ corresponds to a cross section of $\sim 0.1\,\mathrm{nb}$ for resonant muon-pair production. Therefore, the luminosity is determined from Bhabha events for the data points of the $\Upsilon(3S)$

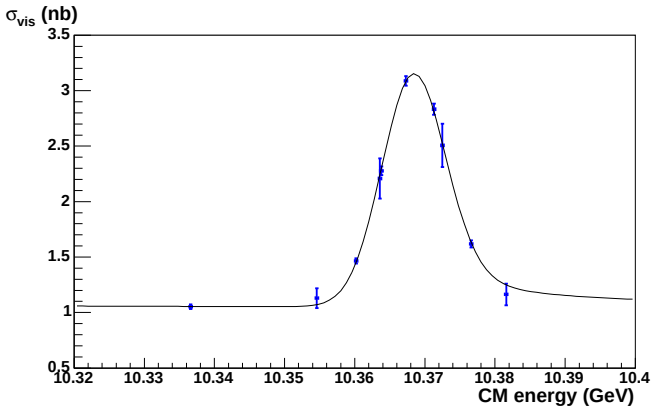

FIG. 3: Visible cross section after event selection vs. the uncorrected CM energy for the $\Upsilon(3S)$ resonance scan. The line is the result of a fit.

scan. Figure 3 shows the data points and the result of a fit.

The Breit-Wigner function (1) of the $\Upsilon(3S)$ resonance is approximated by a delta function because the width of the $\Upsilon(3S)$, $\Gamma^{3S}_{\rm tot} = (26.3 \pm 3.4)$ keV [15], is very small compared to the energy spread of PEP-II. The cross section is related to the visible cross section via equation (9), which is fitted to the data points. The free parameters of the fit are the $\Upsilon(3S)$ mass M^{fit}_{3S}, the energy spread Δ, the parameter P describing the background, and $\varepsilon\frac{\Gamma_{ee}\Gamma_{\rm had}}{\Gamma_{\rm tot}}$, where ε is the efficiency for selecting $\Upsilon(3S)$ decays. The result of the fit including the statistical errors are

$$\begin{aligned} \Delta &= (4.44 \pm 0.09)\,\text{MeV}, \\ M^{\rm fit}_{3S} &= (10367.98 \pm 0.09)\,\text{MeV}/c^2, \end{aligned}$$

with $\chi^2/\text{dof} = 2.2/6$. Sources of a systematic uncertainty in the fit results are potential variations of the detector and trigger performance during the $\Upsilon(3S)$ scan and the precision (± 0.20 MeV) of the determination of the energy differences between the scan points. In total, the systematic uncertainty is estimated to be 0.17 MeV and 0.15 MeV/c^2 for the energy spread and $\Upsilon(3S)$ mass, respectively.

The observed shift of 0.12% between the fitted $\Upsilon(3S)$ mass $M^{\rm fit}_{3S}$ and the world average of (10355.2 ± 0.5) MeV/c^2 [16] is used to correct the PEP-II CM energies. The machine energy spread is extrapolated to 10580.0 MeV/c^2 by scaling the spread of the high-energy beam with the square of its energy, resulting in $\Delta = (4.63 \pm 0.20)$ MeV. An extrapolation of the spread of the low-energy ring is not necessary, because its energy was held constant. The energy spread during two of the three $\Upsilon(10580)$ scans was 0.2 MeV larger. This larger spread was caused by a wiggler that ran at full power till late February 2000. Since this date it runs at only 10% of its full power, which reduces its influence on the spread.

D. The $\Upsilon(10580)$ Peak Cross Section

The $b\bar{b}$ cross section at the peak of the $\Upsilon(10580)$ resonance is determined from the energy dependence of $\sigma_{b\bar{b}}$ measured from a high-statistics data set. These data were taken between October 1999 and June 2002 close to the peak, at energies between 10579 and 10582 MeV. They comprise an integrated luminosity of 76 fb^{-1}, much larger than the typical 0.01 fb^{-1} of a scan. The cross section $\sigma_{b\bar{b}}$ is given by

$$\sigma_{b\bar{b}} = \frac{N_{\rm had} - N_{\mu\mu} \cdot R_{\rm off} \cdot r}{\varepsilon'_{b\bar{b}} L}, \qquad (10)$$

where $N_{\mu\mu}$ is the number of muon pairs, $R_{\rm off}$ is the ratio of hadronic events to muon pairs below the resonance, $\varepsilon'_{b\bar{b}}$ is the efficiency for selecting $B\overline{B}$ events, and r is a factor close to unity, estimated from Monte Carlo simulation, that corrects for variations of cross sections and efficiencies with the CM energy.

We apply cuts on track multiplicity, $N_{\rm ch} \geq 3$, and on the event-shape, $R_2 < 0.5$, to select these hadronic events. Events from $\gamma\gamma$ interactions and beam-gas background are reduced by selecting only events with a total energy greater than 4.5 GeV. Beam-gas interactions are additionally reduced by requiring that the primary vertex of these events lies in the beam collision region.

The peak cross section is determined from this long run on resonance. To take into account the tiny variations of the hadronic cross section close to the maximum, we fit a third-order polynomial to the cross sections $\sigma(e^+e^- \to B\overline{B})$ as a function of uncorrected energy (the energy of the peak position is not used in this analysis, instead the $\Upsilon(10580)$ mass is determined solely from the short-time scans as descibed below). This results in a peak value of $(1.101 \pm 0.005 \pm 0.022)$ nb. The second error is systematic and includes as dominant contributions uncertainties in the efficiency $\varepsilon'_{b\bar{b}}$, calculated from Monte Carlo simulation, and in the luminosity determination.

E. The Three $\Upsilon(10580)$ Scans

The $\Upsilon(10580)$ scan consists of three scans around the resonance mass taken in June 1999, January 2000 and February 2001. Hadronic events are selected by requiring $N_{\rm ch} \geq 4$ and $R_2 < 0.3$. The background from beam-gas and $\gamma\gamma$ interactions is reduced by the cut $E_{\rm tot} - |P_z| > 0.2\sqrt{s}$, where $E_{\rm tot}$ is the total CM energy calculated from all charged tracks and P_z is the component of the total CM momentum of all charged tracks along the beam axis.

The data points $(\sigma^{\rm vis}_i, \sqrt{s_i})$ are listed in Tables I–III. They are shown in Fig. 4 together with a fit based on Eq. (9). The CM energies of the $\Upsilon(10580)$ scans from Jan. 2000 and Feb. 2001 are corrected using the shift obtained from the $\Upsilon(3S)$ fit. This is not possible for the CM energies of the scan from June 1999. In this scan,

TABLE I: Data points of the 1st scan of the $\Upsilon(10580)$ resonance. The cross sections are not efficiency corrected. The energies of this scan are shifted by a constant offset relative to the energy scale of the other two scans. The offset is a free parameter in the simultaneous fit to all three scans. The CM energy spread during this scan was $\Delta = 4.83\,\mathrm{MeV}$.

CM energy (MeV)	σ_{vis} (nb)
10518.2	0.777 ± 0.060
10530.0	0.868 ± 0.048
10541.8	0.828 ± 0.046
10553.7	0.762 ± 0.050
10565.5	0.933 ± 0.044
10571.4	1.203 ± 0.037
10577.3	1.4466 ± 0.0207
10583.3	1.706 ± 0.064
10589.2	1.615 ± 0.122
10595.3	1.291 ± 0.117
10601.3	1.091 ± 0.101

TABLE II: Data points of the 2nd scan of the $\Upsilon(10580)$ resonance. The cross sections are not efficiency corrected. The CM energy spread during this scan was $\Delta = 4.83\,\mathrm{MeV}$. The energy correction obtained from the $\Upsilon(3S)$ scan is applied to the CM energies.

corrected CM energy (MeV)	σ_{vis} (nb)
10539.3	0.9429 ± 0.0282
10571.6	1.452 ± 0.054
10576.7	1.756 ± 0.050
10579.6	1.730 ± 0.044
10584.7	1.650 ± 0.063
10591.4	1.457 ± 0.043
10604.3	1.0686 ± 0.0295

which took several days, it was possible to have the energy drift while data were being collected at a scan point. These drifts have been monitored and the average energies are corrected to $\pm 0.05\,\mathrm{MeV}$, so that point-to-point energy variations are still negligible. The absolute scale, however, can not precisely be calibrated to that of the $\Upsilon(3S)$ scan. For this reason a mass shift between that scan and the later two scans has to be included as a free parameter into the fit. The other free parameters are the total width $\Gamma_{\rm tot} = \Gamma_{\rm tot}(M^2)$, the electronic width Γ_{ee}, the mass M of the $\Upsilon(10580)$ and for each scan the background parameter P and the efficiency $\varepsilon_{b\bar{b}}$. The efficiencies can be free parameters in the fit since we fix the peak cross section for each scan to the value obtained from the on-resonance data set. The energy spread of the collider is fixed to 4.63 MeV for the scan of February 2001 and to 4.83 MeV for the other two scans. Note that the branching fraction $B_{ee} = \Gamma_{ee}/\Gamma_{\rm tot}$ is not an independent parameter. The fit results for the resonance parameters are given in Table VI together with the correlation matrix. The other fit parameters agree with expectations.

TABLE III: Data points of the 3rd scan of the $\Upsilon(10580)$ resonance. The cross sections are not efficiency corrected. The CM energy spread during this scan was $\Delta = 4.63\,\mathrm{MeV}$. The energy correction obtained from the $\Upsilon(3S)$ scan is applied to the CM energies.

corrected CM energy (MeV)	σ_{vis} (nb)
10539.6	0.9775 ± 0.0249
10570.4	1.5236 ± 0.0293
10579.4	1.857 ± 0.040
10579.4	1.850 ± 0.033
10589.4	1.656 ± 0.038

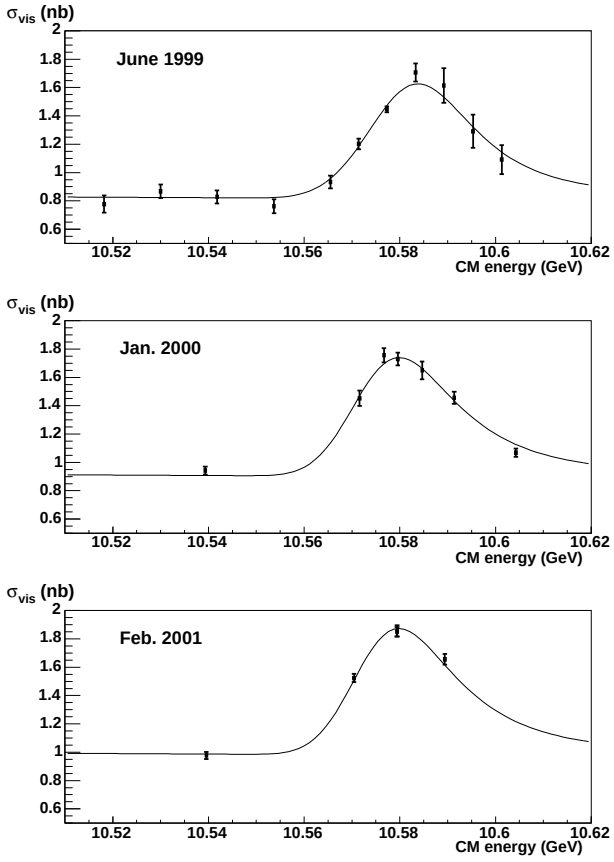

FIG. 4: Visible cross section after event selection vs. CM energy for the three $\Upsilon(10580)$ scans. The lines are the result of a simultaneous fit to all three scans.

F. Systematic Uncertainties

We treat the $\Upsilon(10580)$ resonance as a $4S$ state, but its shape is slightly modified by mixing with the $\Upsilon_1(3D)$ and possibly other states as well as by coupled-channel effects at higher energies above the thresholds for BB^*

TABLE IV: Comparison of the results obtained from a fit to the three $\Upsilon(10580)$ scans using a non-relativistic Breit-Wigner function with an energy independent total decay width (1st row) and the quark-pair-creation model (2nd row) to describe the resonance shape, respectively. The quark-pair-creation model describes the energy dependence of the total decay width close to the open bottom threshold taking spatial features of the $\Upsilon(4S)$ meson wave function into account. We therefore use this model for our measurement, while the fit with a non-relativistic Breit-Wigner function is used as an estimate for the model uncertainties.

	$\Gamma_{\rm tot}$ [MeV]	Γ_{ee} [keV]	$B_{ee} \times 10^5$	M [GeV/c^2]	χ^2/dof
non-rel. Breit-Wigner, $\Gamma_{\rm tot} = {\rm const}$	17.9 ± 1.3	0.288 ± 0.015	1.61 ± 0.04	10.5796 ± 0.0004	15.4/14
quark-pair-creation model	20.7 ± 1.6	0.321 ± 0.017	1.55 ± 0.04	10.5793 ± 0.0004	18.3/14

TABLE V: Summary of systematic uncertainties

	$\delta\Gamma_{\rm tot}$ (MeV)	$\delta\Gamma_{ee}$ (keV)	$\delta B_{ee} \times 10^5$	δM (MeV/c^2)
model uncertainty	1.4	0.017	0.03	0.1
systematic bias by single data point	2.0	0.022	0.04	0.3
uncertainty of energy spread	0.5	0.0024	0.03	< 0.1
uncertainty of peak cross section	< 0.1	0.006	0.03	< 0.1
long term drift of energy scale	-	-	-	1.0
error on $M_{\Upsilon(3S)}$	-	-	-	0.5
total error	2.5	0.029	0.07	1.2

TABLE VI: Central values of the $\Upsilon(10580)$ resonance parameters including their statistical errors and correlation coefficients of the fit to the three $\Upsilon(10580)$ scans. Any combination of two of the three parameters $\Gamma_{\rm tot}$, Γ_{ee} and B_{ee} can be used as free parameters in the fit.

	value obtained from fit	Γ_{ee}	B_{ee}	M
$\Gamma_{\rm tot}$	(20.7 ± 1.6) MeV	0.996	-0.980	0.206
Γ_{ee}	(0.321 ± 0.017) keV		-0.961	0.186
B_{ee}	$(1.55 \pm 0.04) \cdot 10^{-5}$			-0.226
M	(10579.3 ± 0.4) MeV			

and B^*B^* production [17]. An analysis of the energy region around the $\Upsilon(10580)$ that includes all possible states and decay channels is not possible because of the limited energy range of PEP-II and the lack of more detailed theoretical models. Instead, we treat the $\Upsilon(10580)$ as a resonance well enough isolated from other peaks to be described in a model using a pure $4S$ state. This is one reason to omit data taken at CM energies well above the BB^* threshold. Another reason is the fact that details of the meson wave functions become more significant at higher energies, as can be learned from Figure 1.

To estimate the effect of our model we use the width of the resonance shape defined by the full width at half maximum (FWHM) as an alternative definition for $\Gamma_{\rm tot}$. The FWHM is obtained replacing (1) with a non-relativistic Breit-Wigner function with constant width $\Gamma_{\rm tot} = {\rm const}$ in the fit to the data points. This would be the approach when nothing is known about the nature of the resonance. The results are summarized in Table IV. The difference in the fit results tells us the effect of our more refined description. We assume a model uncertainty of 50%, i.e., we take half of the difference for each fit parameter as an estimate of the model uncertainties.

A systematic bias in the fit results could be caused by detector instabilities or an incorrect energy measurement during a scan. This effect is estimated by excluding single data points from the fit. The maximum shift for each fit parameter is taken as a systematic error.

The $\Upsilon(3S)$ scan and the $\Upsilon(10580)$ scans were spread over a period of three years. A systematic error of 1.0 MeV is assigned to the mass measurement due to drifts in the beam energy determination between the $\Upsilon(10580)$ scans and the $\Upsilon(3S)$ scan that are not reflected in the beam energy corrections. These drifts are caused by changes of the beam orbit and ring circumference. Another systematic error on the mass measurement arises from the uncertainty in the mass of the $\Upsilon(3S)$. The systematic error caused by the uncertainty of the energy spread of the collider is estimated by varying the energy spread used in the fit procedure for all three $\Upsilon(10580)$ scans by its uncertainty of ± 0.20 MeV. Long-term fluctuations of the energy spread are taken into account by varying the energy spread of single scans in the fit by ± 0.1 MeV. The quadratic sum of both contributions is listed in Table V. In addition the systematic error due to the uncertainty in the peak cross section is included. The systematic uncertainties due to energy dependences of the event selection efficiencies are found to be negligible.

V. SUMMARY

Our final results are

$$\begin{aligned} \Gamma_{\rm tot} &= (20.7 \pm 1.6 \pm 2.5)\,{\rm MeV}, \\ \Gamma_{ee} &= (0.321 \pm 0.017 \pm 0.029)\,{\rm keV}, \\ B_{ee} &= (1.55 \pm 0.04 \pm 0.07) \cdot 10^{-5}, \\ M &= (10579.3 \pm 0.4 \pm 1.2)\,{\rm MeV}/c^2. \end{aligned}$$

The measurements of the total width and mass are improvements in precision over the current world averages [15].

VI. ACKNOWLEDGMENTS

We appreciate helpful discussions with Alain Le Yaouanc. We are grateful for the excellent luminosity and machine conditions provided by our PEP-II colleagues, and for the substantial dedicated effort from the computing organizations that support *BABAR*. The collaborating institutions wish to thank SLAC for its support and kind hospitality. This work is supported by DOE and NSF (USA), NSERC (Canada), IHEP (China), CEA and CNRS-IN2P3 (France), BMBF and DFG (Germany), INFN (Italy), FOM (The Netherlands), NFR (Norway), MIST (Russia), and PPARC (United Kingdom). Individuals have received support from the A. P. Sloan Foundation, Research Corporation, and Alexander von Humboldt Foundation.

[1] ARGUS Collaboration, H. Albrecht *et al.*, Z. Phys. **C65** 619 (1995).
[2] CLEO Collaboration, D. Besson *et al.*, Phys. Rev. Lett. **54**, 381 (1985).
[3] CLEO Collaboration, C. Bebek *et al.*, Phys. Rev. **D36**, 1289 (1987).
[4] CUSB Collaboration, D. M. Lovelock *et al.*, Phys. Rev. Lett. **54**, 377 (1985).
[5] PEP-II: An Asymmetric B Factory. Conceptual Design Report, SLAC-R-418, LBL-PUB-5379 (1993).
[6] U. Wienands *et al.*, IEEE Proc. of the 1995 Particle Accelerator Conference and International Conference on High-energy Accelerators, Dallas, Texas, May 1995, Piscataway, NJ, IEEE, vol. 1, p. 530–532 (1996).
[7] M. Sullivan, M. Donald, and M. Placidi, IEEE Proc. of the 2001 Particle Accelerator Conference, Chicago, Illinois, June 2001, eds. P. Lucas, S. Webber, Piscataway, N.J., IEEE, 2001, vol. 5, p. 3570–3572 (2001).
[8] *BABAR* Collaboration, B. Aubert *et al.*, Nucl. Instr. and Methods **A479**, 1 (2002).
[9] A. Le Yaouanc, L. Oliver, O. Pene, J.-C. Raynal, Phys. Rev. **D8** 2223 (1973); A. Le Yaouanc, L. Oliver, O. Pene, J.-C. Raynal, Phys. Lett. **B71** 397 (1977); S. Ono, Phys. Rev. **D23** 1118 (1981).
[10] A. Le Yaouanc, priv. communication (1999); h differs by a factor 2 from [1].
[11] E. A. Kuraev, V. S. Fadin, Sov. J. Nucl. Phys. **41**, 466 (1985).
[12] J. P. Alexander, G. Bonvicini, P. S. Drell, R. Frey, Phys. Rev. **D37**, 56 (1988).
[13] D. Albert, J. Marciano, D. Wyler, Z. Parsa, Nucl. Phys. **B166** 460 (1980).
[14] G. C. Fox, S. Wolfram, Phys. Rev. Lett. **41**, 1581 (1978) and Nucl. Phys. **B149**, 413 (1979).
[15] Particle Data Group, S. Eidelman *et al.*, Phys. Lett. **B592**, 1 (2004).
[16] A. S. Artamonov *et al.*, Phys. Lett. **B474** 427 (2000).
[17] K. Heikilä, N. A. Törnqvist, S. Ono, Phys. Rev. **D29**, 110 (1984).